

Toward a Decision Support System for Energy-Efficient Ferry Operation on Lake Constance based on Optimal Control

Hannes Homburger¹, Bastian Jäckl², Stefan Wirtensohn¹, Christian Stopp¹, Maximilian T. Fischer², Moritz Diehl³, Daniel A. Keim², and Johannes Reuter¹

Abstract—The maritime sector is undergoing a disruptive technological change driven by three main factors: autonomy, decarbonization, and digital transformation. Addressing these factors necessitates a reassessment of inland vessel operations. This paper presents the design and development of a decision support system for ferry operations based on a shrinking-horizon optimal control framework. The problem formulation incorporates a mathematical model of the ferry’s dynamics and environmental disturbances, specifically water currents and wind, which can significantly influence the dynamics. Real-world data and illustrative scenarios demonstrate the potential of the proposed system to effectively support ferry crews by providing real-time guidance. This enables enhanced operational efficiency while maintaining predefined maneuver durations. The findings suggest that optimal control applications hold substantial promise for advancing future ferry operations on inland waters. A video of the real-world ferry *MS Insel Mainau* operating on Lake Constance is available at: <https://youtu.be/i1MjCdbEQyE>

I. INTRODUCTION

Recent developments in the field of numerical optimal control, combined with the steadily increasing embedded computing power, enable innovation in autonomy, decarbonization, and digital transformation of inland vessel operation. Pioneered by Gilles and coworkers in the 1990s [1], this innovation can come in the form of advanced optimal control approaches in inland vessel scenarios. Recently, advanced control approaches have been shown to efficiently control vessels autonomously in real-world scenarios [2]. However, regulatory constraints, concerns about safety in edge cases, and questions of economic efficiency currently limit large-scale deployment. In passenger transport, stakeholder trust, explainable system behavior, and profitability are essential factors to achieve real-world impact [3]. These factors are particularly relevant for ferries carrying hundreds of passengers, where there remains a strong preference for a human captain on board. Captains often face challenges when dealing with environmental disturbances such as currents and winds exhibiting non-intuitive characteristics. This motivates the implementation of a decision support system to reduce operator workload and enhance economic efficiency. In this paper, we present the design of a decision support system for the commercial electric ferry *MS Insel Mainau* capable of transporting up to 300 passengers on Lake Constance.

¹ Institute of System Dynamics, HTWG Konstanz, 78462 Konstanz, Germany, hhomburg@htwg-konstanz.de

² Department of Computer and Information Science, University of Konstanz, 78464, Konstanz, Germany

³ Department of Microsystems Engineering (IMTEK) and Department of Mathematics, University of Freiburg, 79110 Freiburg, Germany

A. Contributions

The following main contributions toward energy-efficient operation are presented in this paper:

- **Shrinking-Horizon Optimal Control for Real-World Ferry Operation:** A novel decision support system is proposed based on a shrinking-horizon optimal control problem formulation, which incorporates environmental influences such as water currents and wind. The system employs an efficient direct optimal control approach suitable for providing real-time solutions.
- **Digital Twin of the Ferry and Environmental Disturbances:** A comprehensive mathematical model of the fully-electric ferry *MS Insel Mainau* is developed, including parameter identification and evaluation. Additionally, an optimization-friendly model architecture for current and wind disturbances is selected and validated using data from a PDE-based model.
- **Implementation of the Decision Support System:** The system plans energy-optimal trajectories with respect to the environmental conditions, preserving predefined maneuver durations. This illustrates the potential to support ferry crews with actionable guidance, highlighting the method’s practical feasibility for real-world deployment.

A schematic visualization of the proposed architecture of the decision support system is provided in Fig. 1.

B. Requirements and Related Work

To increase the efficiency of vessel operations and reduce emissions, replacing conventional marine fuel with alternatives [4] or reducing operation speed [5] are prevalent measures. Complementarily, numerical optimization is a promising tool for further improving ferry operations [6], particularly in tough environmental conditions [7]. The primary objective of the decision support system design is to provide the crew with valuable information and insights. Besides an intuitive visualization of the most important processing data, suggestions for the optimal route and velocity profile are essential to the crew. These suggestions should consider the dynamics of the ferry and the following **requirements**:

- Stay in the permitted corridor.
- End at the docking pose at the scheduled time.
- Minimize required energy.

The successful fulfillment of these requirements is essential to ensure acceptance by crew, thereby enabling meaningful real-world impact [3].

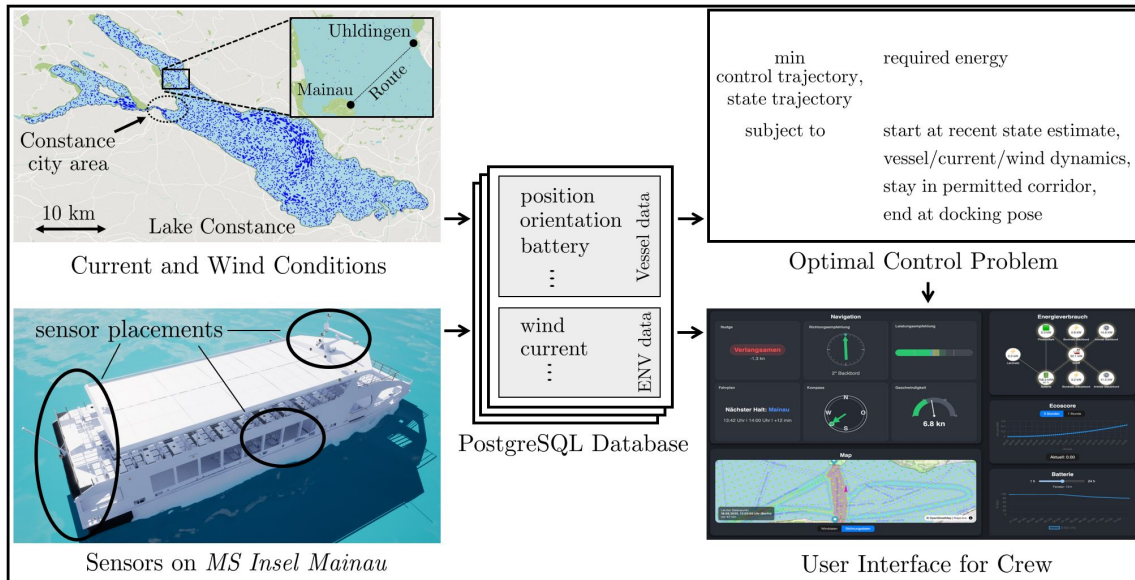


Fig. 1: Schematic architecture of the decision support system for the real-world ferry *MS Insel Mainau*, illustrating the sequential flow from data collection (left), through data storage and management (center), to optimization and visualization modules (right).

A **selection of related work** is given by the following research projects considering (semi-)autonomous real-world ferries. Important examples are the Zeabuz project in Stockholm [8], the autonomous ferry prototypes milliAmpere [9] and milliAmpere2 [10] from NTNU in Norway, the GreenHopper [11] from DTU in Denmark, the German projects CAPTN with the prototype *MS WaveLab* [12] in Kiel, and the Akoon project with the river ferry *Horst* in Ingelheim [13]. **Weather-routing** tools for vessel operation range from tree-search methods [14] over dynamic programming [13] to A*-based algorithms [15]. Empirical evidence for ocean freight indicates that weather routing can yield considerable fuel savings [14]. A comprehensive survey of weather-routing systems for vessels is provided in [16]. In contrast to previous studies, we propose a system designed for inland waterway operation characterized by limited route length and fixed duration. This setting enables a novel, environment-aware direct optimal control formulation, which includes a dynamic ferry model and potentially provides more interpretable and efficient suggestions.

C. Outline

In Section II, an overview of the system is given and the shrinking-horizon optimal control problem is stated, which is the basis for the decision support system. This is followed by a presentation of the ferry's dynamics, the power model, and the limited operation corridor. To simplify the vessel dynamics, observations from real-world operation of the ferry *MS Insel Mainau* are collected and exploited. Section III presents the numerical results based on real-world data. The validation contains a descriptive data analysis of the environmental conditions, an empirical parameter identification of the ferry model, and two illustrative case study scenarios. Finally, Section IV concludes the paper and discusses ideas for future work.

II. ARCHITECTURE OF THE SUPPORT SYSTEM

To meet the requirements defined in the previous section, the decision support system is implemented in the modules data collection, data storage and management, optimization, and visualization. A schematic illustration of the architecture is given in Fig. 1. Data collection comprises 92 data streams on the *MS Insel Mainau*, recorded at 5-second intervals in a PostgreSQL database. The processing data of the ferry is measured using mounted sensors, most prominent:

- Pose, including GPS-position and angular orientation.
- Propellers, including speed, orientation, and power.
- Energy flow, including state of charge of the batteries and solar power supply.

Additionally, hourly current and wind data on Lake Constance are tracked. Those are calculated by the numerical solution of a system of partial differential equations (PDEs) presented in previous work [17]. Selected data is visualized in a user interface (UI) for the captain and also fed into an optimal control problem, which predicts energy-efficient trajectories under the given constraints. The resulting trajectories and self-explanatory nudges are then visualized. In the next part, we detail the optimal control problem formulation.

Optimal Control Problem (OCP) Formulation

To compute optimal input and state trajectories for ferry maneuvers, the defined requirements are embedded in the shrinking-horizon OCP:

$$\underset{u(\cdot), x(\cdot)}{\text{minimize}} \quad \int_t^T P(u(\tau)) + \|Sx(\tau)\|_Q^2 + \|u(\tau)\|_R^2 d\tau \quad (1a)$$

$$\text{subject to} \quad x(t) - \hat{x}_t = 0, \quad (1b)$$

$$x(T) - x_{\text{Dock}} = 0, \quad (1c)$$

$$\dot{x}(\tau) - f(x(\tau), u(\tau), \xi) = 0, \quad \text{for } t \leq \tau \leq T, \quad (1d)$$

$$h(x(\tau), u(\tau)) \leq 0, \quad \text{for } t \leq \tau \leq T. \quad (1e)$$

the actuator force sway direction Y_a , and the turn rate of the vessel \dot{r}_{bf} , yielding the control input $u = [X_a, Y_a, \dot{r}_{bf}]^\top$, and the dynamics are simplified to

$$\dot{\eta} = J_\psi(\eta)v, \quad (3a)$$

$$\dot{v} = \begin{bmatrix} m^{-1} \left(\begin{bmatrix} X_a \\ Y_a \end{bmatrix} + \tilde{\tau}_w(\eta, v, \xi) - \tilde{C}(v)v - \tilde{D}(\eta, v, \xi) \right) \\ \dot{r}_{bf} \end{bmatrix}, \quad (3b)$$

where the terms superscripted by \sim contain the first and second elements of the corresponding terms without the superscript. The simplified ODE system (3) can be rewritten in the standard form $\dot{x} = f(x, u, \xi)$ using the state vector $x = [\eta^\top, v^\top]^\top \in \mathbb{R}^6$ and is part of the shrinking-horizon OCP (1d).

C. Local current and wind model

As discussed at the beginning of this section, the environmental conditions are collected in the form of the numerical solution of a system of PDEs [17]. This numerical solution is given for the entire surface area of Lake Constance in the form of tabular data tuples with entries in the form of

$$[x_1, y_1, v_x, \text{wind}, v_y, \text{wind}, v_x, \text{current}, v_y, \text{current}]^\top \in \mathbb{R}^6. \quad (4)$$

This representation of the environmental conditions is simple but not optimization-friendly in the sense that first- and second-order derivatives are not provided. Further, as depicted in the upper left illustration in Fig. 1, the ferry operates only in a limited area of Lake Constance. Therefore, a local model of the environmental conditions, even providing first- and second-order information, is a key element for efficient optimization. For this aim, a spatial second-order model is chosen and specified as

$$\begin{bmatrix} v_x(x_1, y_1) \\ v_y(x_1, y_1) \end{bmatrix} = \begin{bmatrix} \frac{1}{2}p^\top Q_x p + L_x p + \mu_x \\ \frac{1}{2}p^\top Q_y p + L_y p + \mu_y \end{bmatrix}, \quad (5)$$

where $p := [x_1, y_1]^\top$ is the 2D-position on the water and $Q_x, Q_y \in \mathbb{R}^{2 \times 2}$, $L_x, L_y \in \mathbb{R}^{1 \times 2}$, and $\mu_x, \mu_y \in \mathbb{R}$ contain the parameters. Since Q_x and Q_y can be assumed symmetric without loss of generality, the quadratic models of the 2D current field and 2D wind field require 12 independent parameters each. Consequently, the total number of parameters is $n_\xi = 24$. Note that the introduced spatial quadratic models are optimization-friendly and have low complexity.

Environmental effects on the vessel dynamics: The hydrodynamic damping effects are modeled in \tilde{D} and the force vector by the relative motion in a wind field is $\tilde{\tau}_w$, both dependent on the parameter vector ξ . In detail, the relative velocity to the surrounding water contain the components $u_{r, \text{water}}, v_{r, \text{water}}$ with AoA $\gamma_{r, \text{water}}$ and the relative velocity to the surrounding air is given by the components $u_{r, \text{wind}}, v_{r, \text{wind}}$ with AoA $\gamma_{r, \text{wind}}$. To model the hydrodynamic damping effects, we choose a second-order modulus model given in [19, Sec. 4]. To model the wind effects, a standard wind

model [18, Sec. 10] given by

$$\tilde{\tau}_w = \frac{1}{2}\rho (u_{r, \text{wind}}^2 + v_{r, \text{wind}}^2) \begin{bmatrix} -c_x \cos(\gamma_{r, \text{wind}}) A_{Fw} \\ c_y \sin(\gamma_{r, \text{wind}}) A_{Lw} \end{bmatrix}$$

is employed, where ρ is the air density, $c_x, c_y \in [0, 1]$ are drag coefficients, and $A_{Fw}, A_{Lw} > 0$ are projected areas. Note that no torque is considered in this model, as we assume direct control over the vessel's turn rate in Eq. (3b).

D. Power model

The power required by the actuators of the ferry is

$$P(u) = 2c_p |n_{AT}^3|,$$

where $c_p > 0$ is a coefficient and $n_{AT} := n_{AT,1} = n_{AT,2}$ are the propeller speeds of the azimuth thrusters (AT) required to provide the forces X_a and Y_a , respectively. Using the simplified control allocation, we obtain $4F_{AT}^2 = X_a^2 + Y_a^2$. By ignoring efficiency changes given by slip due to the ferry's moderate velocity, the relation $F_{AT} \propto n_{AT}^2$ holds and

$$P(u) = 2\check{c}_p \left(\frac{1}{4}(X_a^2 + Y_a^2) \right)^{\frac{3}{4}}$$

is obtained, where the ferry-dependent coefficients are collected in the parameter $\check{c}_p > 0$.

E. Path constraints

The path constraints are used to limit the operation corridor and to keep the inputs within a reasonable range. To limit the operation area, we define a convex set of admissible 2D-positions by introducing $i = 1, 2, \dots, I$ linear inequality constraints given by $h_i(x) = s_i x_1 + q_i y_1 + c_i \leq 0$ with parameters $s_i, q_i, c_i \in \mathbb{R}$. Further, to limit the force of the azimuth thruster, the constraint $h_u(u) = X_a^2 + Y_a^2 - \bar{F}_{AT}^2 \leq 0$ is chosen. Based on the introduced functions, the path constraints are

$$h(x, u) = [h_1(x), \dots, h_I(x), h_u(u)]^\top.$$

The resulting operation corridor for the scenario considered in the next section is visualized in Fig. 4. Note that the constraints can be adapted easily to other scenarios.

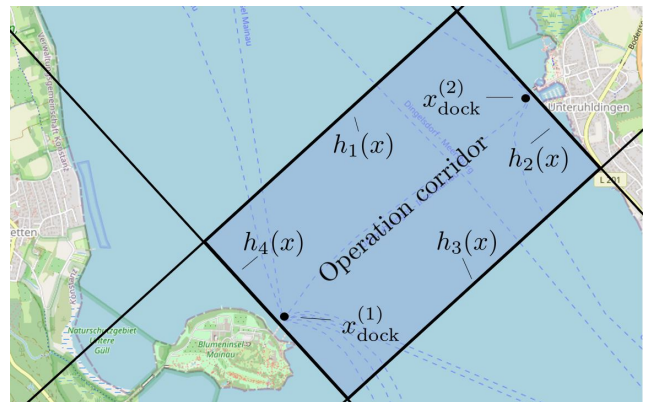


Fig. 4: Map of the upper part of Lake Constance overlaid with the operation corridor including the docking positions. Map data ©2025 OpenStreetMap contributors, licensed under ODbL.

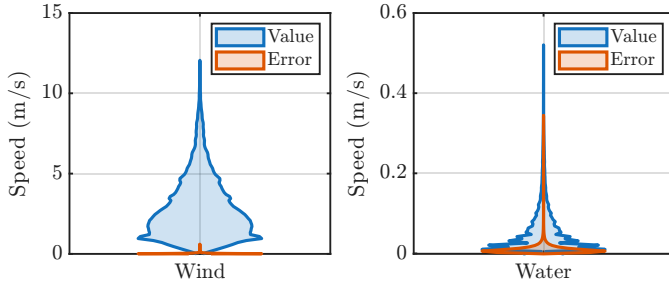


Fig. 5: Violin plots of the PDE modeled current and wind speeds at the operation corridor and the errors of the simplified models.

III. IDENTIFICATION AND NUMERICAL RESULTS

The different parts of the shrinking-horizon OCP are parameterized and identified in this section. Finally, a numerical solution approach and a simulation study are presented.

A. Wind and current model

The spatial quadratic models of the current and wind conditions (5) exhibit lower complexity compared to the tabular data representation (4). To assess whether these models are adequate for capturing the environmental conditions, a descriptive data analysis of the historical wind and current conditions within the operation corridor, along with the corresponding model errors, is conducted. In total, over 2.1×10^6 data points are analyzed between November 3, 2024, and September 9, 2025. The results are summarized in the violin plots shown in Fig. 5. The maximum observed wind speed is 11.7 m/s, corresponding to a Beaufort scale value of 6. The quadratic wind model yields a maximum deviation of 0.52 m/s. The water current velocity does not exceed 0.51 m/s, and detailed analysis reveals that 98.7% of the water model data points exhibit errors below 0.05 m/s. The wind model shows higher accuracy relatively because it is unaffected by coastal influences, unlike the water currents. The empirical results indicate that quadratic models are suitable choices in the given operating corridor.

B. Empirical parameter identification

The determined parameters of the dynamic model of the ferry *MS Insel Mainau* are listed in Table I. Linear and quadratic hydrodynamic damping coefficients are determined to match real-world measurements in least squares (cf. Fig. 6) in surge direction. The projected areas of the vessel are determined by its overall length of 30 m, width of 8.1 m, and height of 7.3 m. The aerodynamic drag terms are determined by assuming an ellipsoidal body for the frontal effects and a cube with reduced height for the side effects [20, Sec. 3]. Note that these parameters match the rough suggestion for vessel drag coefficients in [18, Ch. 10] and, if necessary,

TABLE I: Identified parameters of the *MS Insel Mainau*.

	Hydrodynamic	Wind	Other
X_u	1470 Ns/m	A_{Fw} 59.2 m ²	m 35000 kg
X_{uu}	753 Ns ² /m ²	A_{Lw} 219 m ²	\bar{F}_{AT} 24000 N
Y_v	10290 Ns/m	c_x 0.59 (-)	ρ 1.204 kg/m ³
Y_{vv}	5272 Ns ² /m ²	c_y 0.84 (-)	\check{c}_p 0.0417 m ^{1/2} kg ^{-1/2}

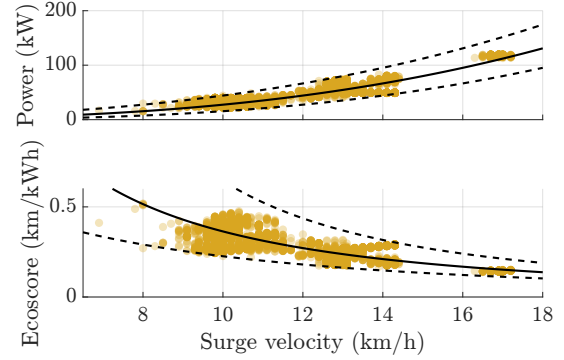


Fig. 6: Power and *ecoscore* of ferry *MS Insel Mainau* over static surge velocity with parameters given in Table I (black), dashed lines under uncertainties, and measured real-world data (gold).

can be optimized by a detailed computational fluid dynamics (CFD) study. The power parameter \check{c}_p is fitted with least-squares to real-world data. Finally, the mass m , the maximum force \bar{F}_{AT} , and the air density ρ are prior known.

C. Solution method and numerical results

The OCP is transcribed in a nonlinear program (NLP) by direct multiple shooting [21]. The NLP is implemented via CasADi [22] and solved with IPOPT [23]. For integration, the explicit Runge-Kutta method of 4th-order is employed. To illustrate the results, we consider two scenarios.

Scenario 1: This scenario demonstrates the decision support in standard operation. For a wind speed of 11 m/s and spatially varying currents with amplitude 0.1 m/s, the suggested trajectory with remaining $T - t_1 = 240$ s is shown in Fig. 7 in black. Since the crew deviates from the initial plan, the trajectory is updated sequentially. The updated trajectory suggested for $T - t_2 = 120$ s is plotted in gold. Both trajectories also include yaw angles and velocity profiles that support environment-aware and energy-efficient operation.

Scenario 2: A simulation study is conducted to examine the impact of environmental conditions and maneuver time on the energy required for the dock-to-dock transfer. A distance of 2527 m separates the docking positions (cf. Fig. 4). The Pareto fronts obtained with the proposed method

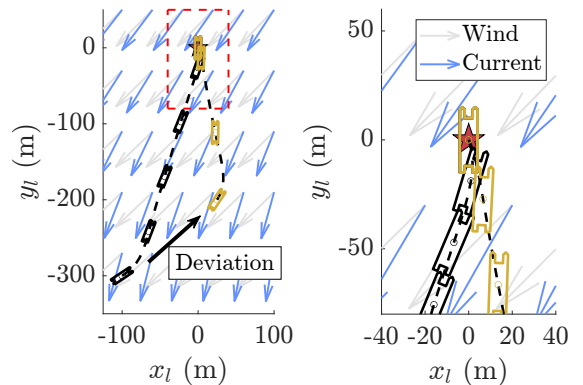


Fig. 7: Optimized ferry routes over the wind field and the current field with zoom on the right. The coordinate system is shifted and rotated to achieve $x_{\text{dock}}^{(1)} = [0, 0, \pi/2]^T$ for visualization.

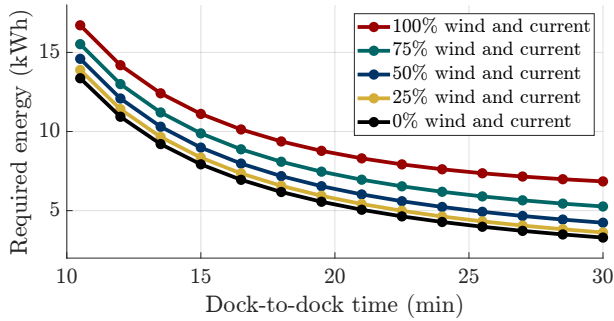


Fig. 8: Pareto fronts given by required energy over maneuver time for different environmental conditions in *Scenario 2*.

are shown in Fig. 8. Both the wind and the current are directed from the north, where 100% corresponds to a wind speed of 13 m/s and a current speed of 0.2 m/s. The required energy increases with shorter dock-to-dock time and stronger environmental disturbances. This information can guide future time scheduling in ferry operations. For reproducibility, the full implementation is available at: <https://github.com/hhomb/Ferry>

IV. CONCLUSION

This paper presents the design of a decision support system for the real-world ferry *MS Insel Mainau* based on a dynamic model. The presented approach is formulated as a shrinking-horizon optimal control problem, demonstrating the potential of embedded numerical optimization as a powerful tool for developing semi-autonomous ferries that prioritize energy efficiency while fulfilling several additional requirements. The real-world data indicate a high potential to save energy through environment-aware trajectory optimization. The resulting optimal control problem is solved numerically using a direct approach, and the solution trajectory meets the specifications. In future work, the decision support system can be attempted in the real world, and the results can be compared to the ground-truth with a complete 3-DOF model.

FUNDING AND ACKNOWLEDGMENT

This research was supported by the City of Konstanz' Smart Green City program as part of the "Model Projects Smart Cities" funding program of the German Federal Ministry for Housing, Urban Development and Building (BMWSB) under grant no. KfW 13622889 and DFG via projects 504452366 (SPP 2364) and 525018088. The authors would like to thank Bodensee Schifffahrtbetriebe (BSB), with Managing Director Christoph Witte and his team, for making the real-world ferry *MS Insel Mainau* available for our research. Additionally, we appreciate the support of the Environmental Protection Agency of Baden-Württemberg (LUBW) for providing the estimated current and wind data.

REFERENCES

- [1] A. Wahl and E.-D. Gilles, "Track-keeping on waterways using model predictive control," *IFAC Proceedings Volumes*, vol. 31, no. 30, pp. 149–154, 1998.
- [2] S. J. N. Lexau, M. Breivik, and A. M. Lekkas, "Automated docking for marine surface vessels—a survey," *IEEE Access*, vol. 11, pp. 132 324–132 367, 2023.

- [3] M. Lützhöft and J. Earchy, Eds., *Human-Centred Autonomous Shipping – Autonomous shipping revisited*. Taylor & Francis, 2024, doi:10.1201/9781003430957-7.
- [4] E. A. Bouman, E. Lindstad, A. I. Riialand, and A. H. Strømman, "State-of-the-art technologies, measures, and potential for reducing GHG emissions from shipping – a review," *Transp. Research Part D: Transport and Environment*, vol. 52, pp. 408–421, 2017.
- [5] A. U. Schubert, R. Damerius, and T. Jeinsch, "Energy demand of vessels depending on current wind conditions," in *2024 European Control Conference (ECC)*. IEEE, 2024, pp. 1147–1152.
- [6] J. Barreiro, S. Zaragoza, and V. Diaz-Casas, "Review of ship energy efficiency," *Ocean Engineering*, vol. 257, p. 111594, 2022.
- [7] H. Homburger, S. Wirtensohn, M. Diehl, and J. Reuter, "Energy-optimal planning and shrinking horizon MPC for vessel docking in river current fields," in *2024 European Control Conference (ECC)*. IEEE, 2024, pp. 1125–1130.
- [8] H. W. Hjelmeland, B.-O. H. Eriksen, O. J. Mengshoel, and A. M. Lekkas, "Identification of failure modes in the collision avoidance system of an autonomous ferry using adaptive stress testing," *IFAC-PapersOnLine*, vol. 55, no. 31, pp. 470–477, 2022.
- [9] M. Hinostrroza, C. Fruzzetti, A. Gudahl Tufte, S. J. N. Lexau, A. Gusev, E. Eide, E. F. Brekke, A. M. Lekkas, R. Skjetne, M. Martelli, and M. Breivik, "Model identification, dynamic positioning, and thrust allocation system for the milliamperel autonomous ferry prototype: Field trial results," *IEEE Access*, vol. 13, pp. 133 609–133 634, 2025.
- [10] O. A. Alsos, M. Saghafian, E. Veitch, F.-M. Petermann, T. A. Sitompul, J. Park, E. Papachristos, E. Eide, M. Breivik, and Ø. Smogeli, "Lessons learned from the trial operation of an autonomous urban passenger ferry," *Transp. Research Interdis. Persp.*, vol. 26, p. 101142, 2024.
- [11] T. T. Enevoldsen, M. Blanke, and R. Galeazzi, "Sampling-based collision and grounding avoidance for marine crafts," *Ocean Engineering*, vol. 261, p. 112078, 2022.
- [12] G. Al-Falouji, L. Haschke, D. Nowotka, and S. Tomforde, "Self-explanation as a basis for self-integration - the autonomous passenger ferry scenario," in *2023 IEEE Int. Conference on Autonomic Computing and Self-Organizing Systems Companion (ACSOS-C)*. IEEE, 2023, pp. 65–70.
- [13] P. Koschorrek, M. Kosch, M. Nitsch, D. Abel, and D. Jürgens, "Towards semi-autonomous operation of an over-actuated river ferry," *at - Automatisierungstechnik*, vol. 70, no. 5, pp. 433–443, 2022.
- [14] M. Bentin, D. Zastrau, M. Schlaak, D. Freye, R. Elsnér, and S. Kotzur, "A new routing optimization tool-influence of wind and waves on fuel consumption of ships with and without wind assisted ship propulsion systems," *Transp. Research Procedia*, vol. 14, pp. 153–162, 2016.
- [15] M. Grifoll, C. Borén, and M. Castells-Sanabra, "A comprehensive ship weather routing system using CMEMS products and A* algorithm," *Ocean Engineering*, vol. 255, 2022.
- [16] T. P. Zis, H. N. Psaraftis, and L. Ding, "Ship weather routing: A taxonomy and survey," *Ocean Engineering*, vol. 213, p. 107697, 2020.
- [17] U. Lang, R. Schick, and G. Schröder, "The decision support system BodenseeOnline for hydrodynamics and water quality in Lake Constance," in *Decision Support Systems Advances*, G. Devlin, Ed. InTech, 2010. [Online]. Available: <https://www.lubw.baden-wuerttemberg.de/wasser/bodenseeonline>
- [18] T. I. Fossen, *Handbook of marine craft hydrodynamics and motion control*, 2nd ed. West Sussex: Wiley, 2021.
- [19] H. Homburger, S. Wirtensohn, P. Hoher, T. Baur, D. Griesser, M. Diehl, and J. Reuter, "Solgenia—a test vessel toward energy-efficient autonomous water taxi applications," *Ocean Engineering*, vol. 328, p. 121011, 2025.
- [20] S. F. Hoerner, *Fluid-dynamic Drag: Practical Information on Aerodynamic Drag and Hydrodynamic Resistance*. Hoerner Fluid Dynamics, 1965.
- [21] H. G. Bock and K. J. Plitt, "A multiple shooting algorithm for direct solution of optimal control problems *," *IFAC Proceedings Volumes*, vol. 17, no. 2, pp. 1603–1608, 1984.
- [22] J. A. E. Andersson, J. Gillis, G. Horn, J. B. Rawlings, and M. Diehl, "CasADI: a software framework for nonlinear optimization and optimal control," *Mathematical Programming Computation*, vol. 11, no. 1, pp. 1–36, 2019.
- [23] A. Wächter and L. T. Biegler, "On the implementation of an interior-point filter line-search algorithm for large-scale nonlinear programming," *Mathematical Programming*, vol. 106, no. 1, pp. 25–57, 2006.